Deformation of fluid fronts in a gap-modulated Hele-Shaw cell

Author: Lautaro Díaz Piola
Facultat de Física, Universitat de Barcelona, Martí i Franquès 1, 08028 Barcelona, Spain.

Advisors: Jordi Ortín and Ramon Planet
Departament de Física de la Matèria Condensada

We have studied experimentally the morphology and dynamics of stable oil-air displacements in a gap-modulated Hele-Shaw cell, in the case where the modulation is persistent in the direction of front advancement. Local changes in capillary pressure result in non-local deformations of the two-phase fronts, which have been recorded with a high speed camera and digitized in space and time. The front morphologies observed experimentally in the steady state are in excellent agreement with the predictions of a linear theory, particularly for low intensities of the gap modulation and for both positive and negative modulations. We have also studied the spatio-temporal dynamics of deformation of a nearly initially flat front towards the steady state. In the presence of a positive modulation of the gap thickness, the difference in height between the front tip at the central modulation of the cell and its lateral tails accelerates in time, following $h_{max} \sim t^{1/4}$.

I. INTRODUCTION

Understanding fluid flow in disordered media is of great interest because it is present in diverse phenomena like soil irrigation, oil recovery, printing or fluid transport in plants [1]. In the case where a more wetting fluid displaces a less wetting one the process is known as imbibition. This displacement is stable when the displacing fluid is more viscous than the displaced one. From a fundamental point of view stable imbibition in disordered media has been widely studied as a dynamical non-equilibrium process leading to rough interfaces [2, 3]. The morphology of an imbibition front in a heterogeneous medium is the result of the local variations of capillary pressure and permeability.

The origin of capillary phenomena is in surface tension γ, defined as the energy G needed to increase the surface area A between two fluids by one unit $\gamma \equiv (\partial G/\partial A)_{p,T,n}$. From a thermodynamic point of view it is clear that fluids tend to minimize their surface area to minimize their surface energy [4]. Capillary force can become dominant over other volumic forces like gravity when we reduce the lenght scales of our system, and it can be one of the main contributions that determines the fluid flow dynamics. As an example of a field where capillarity is relevant we encounter microfluidics (submillimiter-sized sistems), that has gained a lot of attention in the last years since the possibility of lab-on-a-chip technological applications are appealing [5]. Viscous forces are also crucial to understand the behaviour of fluid interfaces. In the large friction limit fluid flow is governed by Darcy's law, which states that the flow rate is proportional to the applied pressure gradient. The coefficient of proportionality depends on a geometric property of the medium (its permeability, which has dimensions of lenght sqared) and on the dynamic viscosity μ of the fluid. The relative importance of viscous to capillary forces is measured by the capillary number, defined as $Ca = \mu V/\gamma$, where V is the average velocity of the fluid at the inlet.

A real disordered medium contains numerous defects with a wide distribution of sizes. The aim of the present report is to study the effect of single heterogeneities. Interestingly, the single defect problem has been investigated in other fields. One of them is in the dynamics of wetting, where the motion of a contact line is studied for the case when it interacts with only one defect [6–8]. Another relevant case where the single heterogeneity is discussed is in the dynamics of crack fronts, where nonlinear behaviour was identified experimentally in the dynamics of the crack [9]. These two examples have different physical origins, but it's interesting to remark that under certain assumptions they can lead to similar dynamic equations.

In order to study the effect of single heterogeneities in imbibition processes we use a Hele-Shaw (HS) cell with a gap modulation in the transverse direction to the fluid propagation. This gap modulation introduces simultaneously variations in capillary pressure and in the permeability of the medium. The evolution equation of an interface in a gap modulated HS cell has been derived analytically in [10, 11]. We will compare this theoretical result of the interface morphology with our experiments. In particular, we will analyse the role of the gap spacing and study the interplay between capillarity and permeability.

II. EXPERIMENTAL SETUP

A Hele-Shaw cell consists of two parallel plates separated by a narrow gap b_0. Our cell has a top glass plate and a bottom fiberglass plate and its dimensions are $L_x \times L_y = 190 \times 500$ mm. The plates are separated by a rectangular PVC frame. Its purpose is to impose a well controlled gap spacing b_0 and also to close the cell hermetically. In our experiment we modified the gap parameter b_0, taking different values in the range of (0.26 - 0.66) $\pm$ 0.02 mm.

The gap modulation consists of three equally spaced copper tracks of height $\delta b = 0.06 \pm 0.01$ mm in the bottom plate (see Fig. 1). Thus the gap takes the values b_0 or $b_0 - \delta b$. The width of the tracks is $w = 3$ mm and the distance between them is $a = 48$ mm. These tracks are parallel to the direction of fluid propagation and this geometry has been obtained using printed circuit technology.

A syringe pump controls the flow rate inside the cell which will be constant in all our experiments $Q = 26$ mm^3/s. The fluid used is the silicon oil Rhodorsil 47V, adequate for this type of experiments because of its high wettability, i.e. low contact angle $\theta_c \sim 0°$. The oil properties are: kinematic viscosity $\nu = 50$ mm^2/s, density $\rho = 998$ kg/m^3 and oil-air surface tension $\gamma = 20.7$ mN/m at room temperature. The pump drives the oil into the cell, and the oil fills a reservoir before entering between the parallel plates to produce a uniform injection. A complementary system allows us to inject fluid at high pressure in order to get initial flat interfaces.

A high resolution camera with a spatial resolution of 0.19 mm^2/pixel is used to take pictures of the cell at a frame rate of 30 frames per second. With the camera software MotionPro we track the advancing fluid front and through a MatLab code we extract the coordinates of the front $h(x,t)$ for the analysis.

The measurement procedure is as follows: i) with the pump always on, we introduce the oil in the cell through the complementary injection system at high pressure in order to get an initial flat interface, ii) we close the high pressure injection so that only the pump drives the flow, iii) we start the measurements with the camera software. Since our geometry has mirror symmetry in the flow direction with respect to the central track we expect that the interface will be symmetric also. This has been a hard task to achieve since any little perturbation can produce distortions in the front and the above mentioned procedure has to be repeated.

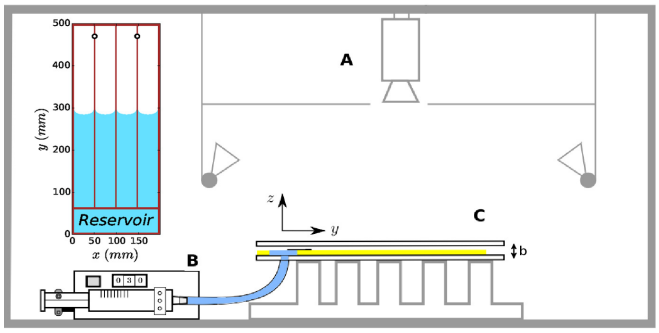

FIG. 1: Basic representation of the experimental setup. **A:** image acquisition system. **B:** syringe pump. **C:** Hele-Shaw cell with bottom and top plates. The oil, represented in blue, displaces the air present in the cell, and the air flows out of it through two holes at the end of the top plate. The cell seen from above with the copper gap modulation is shown as an inset (figure courtesy of Xavier Clotet).

III. THEORETICAL FORMULATION

Most of our experiments are performed in the steady state, that is, when the the interface does not evolve in time. Our motivation to study the steady state is that analytical forms for the front coordinates $h(x)$ have been found in Ref. [11], within a linear approximation $|\partial_x h| \ll 1$. We remark that this analytical solution is deduced for a case where lateral boundary conditions are imposed at infinity, while in our experimental setup the interface is constrained to the dimensions of the cell. The interface equation for this geometry is:

$$h(x) = \int_{\mathbb{R}} dx' \xi(x') G(x - x'). \tag{1}$$

It is written in terms of a propagator $G(x - x')$ and a modulation of the cell gap $\xi(x)$ defined through $b(x) = b_0^2(1 + \xi(x))$ where $b(x)$ is the cell gap at x. It is also assumed that the modulation is smooth, i.e. $|\partial_x b| \ll 1$. For the steady state the propagator has two contributions: one due to capillarity and one due to the permeability of the cell, $G_{steady} \equiv G_{st,cap} + G_{st,per}$, with:

$$G_{st,cap} = \frac{\ell_1}{2\ell_2} e^{-|x|/\ell_2}. \tag{2}$$

$$G_{st,per} = \frac{1}{\pi}\left[\ln|x| + \Gamma + \ln(2\pi) - \frac{1}{2}\left(e^{|x|/\ell_2} Ei\left(-\frac{|x|}{\ell_2}\right) + e^{-|x|/\ell_2} Ei\left(\frac{|x|}{\ell_2}\right)\right)\right]. \tag{3}$$

Here $\ell_1 = b_0(Ca/12)^{-1}$ and $\ell_2 = b_0(Ca/12)^{-1/2}$ are the relevant lenght scales of the system, Γ is the Euler constant and Ei is the exponential integral function [12]. It is interesting to note that the capillary propagator has finite range and thus noise effects due to the gap modulation only propagate for a finite distance along the interface. On the other hand, permeability effects dominate for distances far away from the perturbation. Thus, a perturbation in the cell's gap can give rise to non-local deformations of the fluid front. For the geometry used in our experiments (Fig. 2) the gap modulation is:

$$\xi(x) = \left[\left(\frac{b_0 - \delta b}{b_0}\right)^2 - 1\right] \sum_{n\in\mathcal{Z}} \left[\theta(x - an + \frac{w}{2}) - \theta(x - an - \frac{w}{2})\right]. \tag{4}$$

Where θ are Heaviside functions. In the limit of no modulation $\delta b \to 0$ we have $b^2(x) \to b_0^2$ as expected.

IV. RESULTS

Steady state

To achieve a steady state experimentally in an accurate way we let the fluid front advance for at least half of

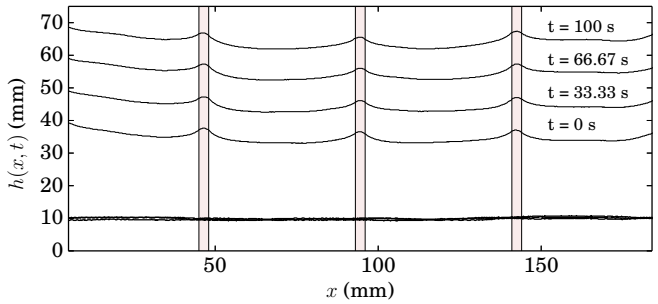

FIG. 2: Morphology of the fluid front and time evolution for a gap $b_0 = 0.46$ mm. The vertical narrow stripes represent the regions where the copper (gap modulation) is present.

the total distance of the cell and we start the measurement after we check that the morphology is not changing in time. In Fig. 2 we show the front for different times with a particular gap $b_0 = 0.46$ mm to illustrate that the morphology remains constant. The flat lines at the bottom result from substracting the y coordinate of consecutive fronts and it is shown that they collapse and no significant time evolution occurs.

Positive modulation

To study the influence of the gap thickness we measured the steady state for diferent values of b_0: 0.26, 0.46, 0.56 and 0.66 mm. The interface morphology for these gaps is shown in Fig. 3. Continuous lines correspond to experimental data and dotted lines to the theoretical prediction. Theoretical data results from integrating equation (1) numerically. At the lateral tails of the front the deviation from the theory is more pronounced because the boundary conditions are different. The oil wets the lateral spacers and, thus, tends to advance preferentially

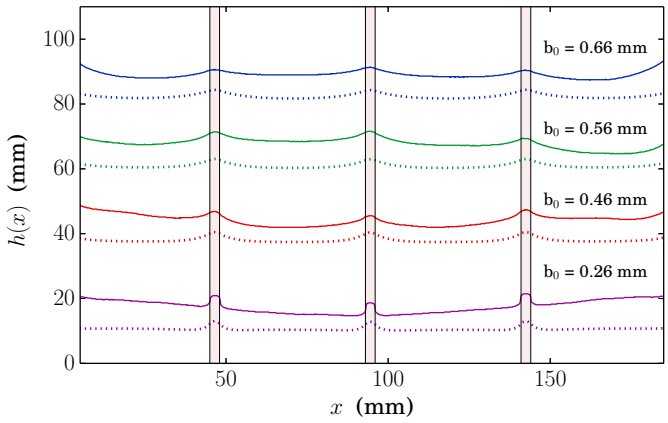

FIG. 3: Steady state morphology of the front for different gap spacings. Continuous lines correspond to experimental data and dotted lines to the analytical solution.

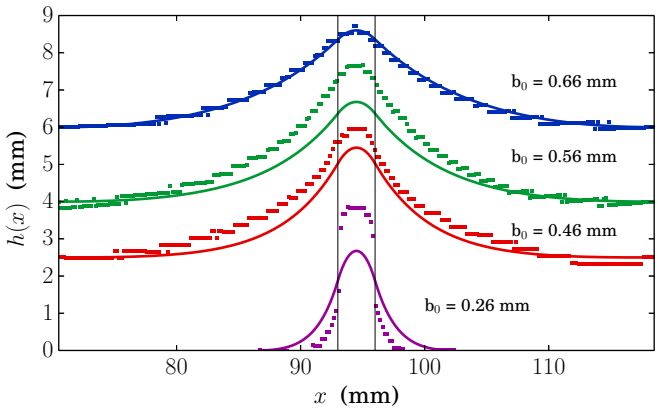

FIG. 4: Steady state morphology of the front for different gap thickness around the heterogeneity. Continuous lines correspond to the analytical solution and dots to experimental data.

along the walls. However, near the central track our measurements show good agreement with the theoretical results particularly at large gap thickness (see Fig. 4). In the areas where the modulation is present variations of capillary pressure cause the peaks in the front morphology. This is consistent with the Young-Laplace condition for the pressure jump across the interface:

$$\Delta p = \gamma \left(\kappa + \frac{2\cos\theta_c}{b(x)} \right), \tag{5}$$

where κ is the curvature in the cell plane and θ_c the contact angle (with $\cos\theta_c = 1$ for perfect wetting). Equation (5) shows that whenever the gap decreases the pressure jump increases. Indeed, as the parameter b_0 decreases the distortion of the morphology is more localized around the heterogeneity. In this case we also notice a marked deviation from the theory because the theory is derived within a linear approximation $|\partial_x h| \ll 1$.

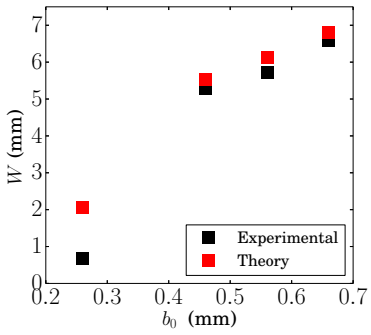

FIG. 5: Normalized width of the theoretical and experimental profiles of Fig. 4.

In order to characterize the morphology of the front distortions, we calculate the normalized width $W = [\langle x^2\rangle - \langle x\rangle^2]^{\frac{1}{2}}$ of the theoretical and experimental profiles

around the track normalized by their mean, $\tilde{h} = h/\langle h \rangle$. The result is shown in Fig. 5. The agreement between theory and experiments is remarkable, since there are no adjustable parameters, and it improves as the gap thickness gets larger as expected.

Negative modulation

We also performed experiments in which the gap modulation was inverted from the one presented before. With this geometry copper is everywhere in the bottom plate except in the three central tracks, as shown in Fig. 6. The tracks now retard the front in stead of making it advance preferentially. A mirror symmetry arises in the morphology when we compare this figure with Fig. 3. This symmetry is not perfect, however, because the gap thickness modulation here is $b_0 - \delta b$ in the wide regions and b_0 in the stripes, while the mirror-symmetric conditions of Fig. 3 would be b_0 in the wide regions and $b_0 + \delta b$ in the stripes.

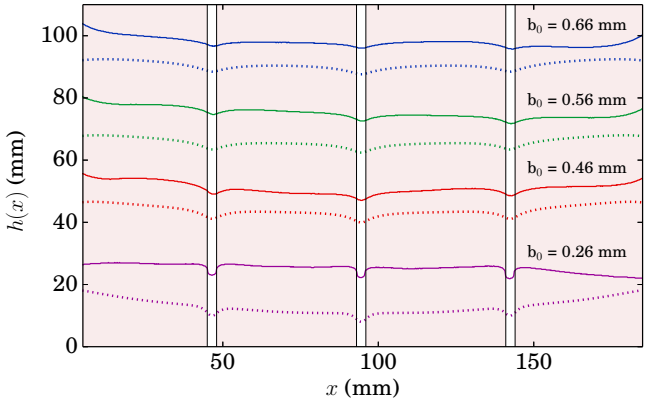

FIG. 6: Steady state morphology of the front for different gap spacings. The vertical white stripes represent the regions where the copper (gap modulation) is not present in the cell. Continuous lines correspond to experimental data and dotted lines to the corresponding analytical solution.

Temporal dynamics

In this section we focus on the temporal dynamics carrying an initially nearly-flat interface towards the steady state. Here we start measuring right after having cut the high pressure injection, and we follow the dynamics of the front in time. Fig. 7 presents the early-time dynamics around the central track for a positive gap modulation. We observe an imbibition dynamics: the region of the meniscus on the track advances much faster than the adjacent tails.

The position h_{max} (the difference in height between the front peak and the front tails) follows very approximately $h_{max} \sim t^{1/4}$, as shown in Fig. 8. This is a slower

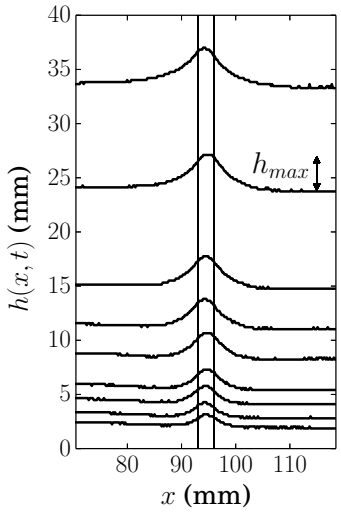

FIG. 7: Early-time dynamics of the fluid front around the central track for a gap thickness $b_0 = 0.46$ mm. From bottom to top the times in the figure are $t = 0,\ 1.67,\ 4.67,\ 8,\ 18,\ 28,\ 41.33,\ 74.67$ and 107.33 s.

dynamics than Washburn's law, $\langle h \rangle \sim t^{1/2}$, that would correspond to the average position of an imbibition front driven by a constant pressure gradient. We argue that the observed dynamics arises from a competition between the capillary suction force and the condition of constant flow rate.

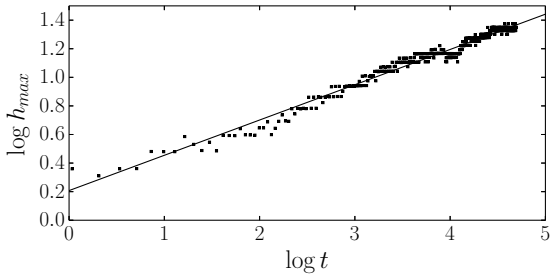

FIG. 8: Log-log plot of the difference in height between the front peak and the front tails, h_{max}, as function of time, for the type of displacements represented in Fig. 7. Solid symbols are experimental values, and the straight line is a power law with exponent 1/4.

V. CONCLUSIONS

We have experimentally studied a stable imbibition displacement, in which a viscous wetting fluid (silicon oil) displaces a less viscous non-wetting fluid (air), in a Hele-Shaw cell with a gap modulation along x, transverse to the fluid front propagation direction. Since the modulation is persistent in this direction the steady state profile of the front can be derived analytically in the linear

approximation, $|\partial_x h| \ll 1$, and for smooth gap modulations, $|\partial_x b| \ll 1$, as reported in Ref. [11].

Experimental results and theoretical predictions in the steady state have been compared for different intensities in the gap modulation $\delta b/b_0$. Positive modulations with narrow stripes and negative modulations with wide stripes have also been studied. In both cases we have observed a remarkable agreement between theory and experiments without any adjustable parameter. This agreement is particularly accurate at low intensities of the modulation for which the linear approximation is more valid. Near from the lateral walls the boundary conditions in the experiment do not correspond with the ones imposed in the theory and thus the differences are understandable. For this reason we designed a modulation geometry that tends to isolate the behaviour of the central track from the behaviour near the walls.

We have also carried out a first study of the spatio-temporal dynamics of an initially nearly-flat front in the gap-modulated cell. The front accelerates locally on the regions of smaller gap thickness. The dynamics of the front tip on the central track has been found to follow a slower dynamics than Washburn's law. This behaviour can be studied theoretically also by numerical integration of the corresponding sharp-interface dynamic equations [11]. The comparison with experiments would be a natural continuation of the present work.

The observed spatio-temporal dynamics is reminiscent of the relaxation of elastic interfaces (contact lines and fracture fronts) previously deformed by the presence of isolated defects [6–9]. This similarity deserves further investigation.

Acknowledgements

I wish to express my sincere gratitude to Jordi Ortín for all the effort, time and interest that he has given on this project. I also want to thank Ramon Planet for his generous contributions and interesting suggestions. I am grateful to my parents and my sister too for all their constant support.

[1] M. Alava, M. Dubé and M. Rost. Imbibition in disordered media. Adv. Phys. **53**, 83 (2004).

[2] J. Soriano *et al.* Anomalous roughening of viscous fluid fronts in spontaneous imbibition. Phys. Rev. Lett. **95**, 104501 (2005).

[3] X. Clotet, J. Ortín and S. Santucci. Disorder-induced capillary bursts control intermittency in slow imbibition. Phys. Rev. Lett. **113**, 074501 (2014).

[4] P.G. de Gennes, F. Brochard-Wyart and D. Quéré (2004). *Capillarity and wetting phenomena. Drops, bubbles, pearls, waves.* Springer.

[5] H. Bruus (2008). *Theoretical Microfluidics.* Oxford Master Series in Physics.

[6] J.F. Joanny and P.G. de Gennes. A model for contact angle hysteresis. J. Chem. Phys. **81**, 552 (1984).

[7] E. Raphaël and P.G. de Gennes. Dynamics of wetting with non-ideal surfaces. The single defect problem. J. Chem Phys. **90**, 7577 (1989).

[8] S. Moulinet, C. Guthmann and E. Rolley. Dissipation in the dynamics of a moving contact line: effect of the substrate disorder. Eur. Phys. J B **37**, 127 (2004).

[9] J. Chopin, A. Prevost, A. Boudaoud and M. Adda-Bedia. Crack front dynamics across a single heterogeneity. Phys. Rev. Lett. **107**, 144301 (2011).

[10] E. Pauné and J. Casademunt. Kinetic roughening in two-phase fluid flows through a random Hele-Shaw cell. Phys. Rev. Lett. **90**, 144504 (2003).

[11] O. Campàs and J. Casademunt. Morphological dynamics of gap-modulated Hele Shaw flows (2002). Internal report.

[12] $Ei(x) = \int_{-\infty}^{x} dt\, e^t/t$.